Tellurium(V). A Pulse Radiolysis Study

U. K. Kläning*,†

Chemistry Department, University of Aarhus, DK-8000 Aarhus C, Denmark

K. Sehested‡

Risø National laboratory, DK-4000 Roskilde, Denmark

Four different tellurium(V) oxoradicals, assumed to be $H_2TeO_4^-$, TeO_3^-, $HTeO_4^{2-}$, and TeO_4^{3-}, were detected by the pulse radiolysis technique. $H_2TeO_4^-$ is the product of the reaction of OH with $HTeO_3^-$, whereas $HTeO_4^{2-}$ and TeO_4^{3-} arise by reactions of OH and O^- with the TeO_3^{2-}. TeO_3^- is a secondary product formed by dehydration of $H_2TeO_4^-$, a process catalyzed by $HTeO_3^-$. The same tellurium(V) species except $H_2TeO_4^-$ are formed by reaction of the hydrated electron with H_6TeO_6, $H_5TeO_6^-$, and $H_4TeO_6^{2-}$. The spectra, kinetics of the reactions of the tellurium(V) species, the acidity constant of $HTeO_4^{2-}$ ($\sim 10^{-13}$), and the apparent acidity constant of TeO_3^- (10^{-10}) have been measured. The standard Gibbs energies of formation $\Delta_f G_{ao}^o(TeO_3^-)$ = −214 kJ/mol, $\Delta_f G_{ao}^o(HTeO_4^{2-})$ = −394 kJ/mol, and $\Delta_f G_{ao}^o(TeO_4^{3-})$ = −319 kJ/mol were determined from the rate constants for the forward and reverse reactions $TeO_3^{2-} + O^- \leftrightarrows TeO_4^{3-}$ and $TeO_3^{2-} + OH \leftrightarrows HTeO_4^{2-}$, combined with the acidity constants of TeO_3^- and $HTeO_4^{2-}$ and the standard Gibbs energy of formation of OH, O^-, and TeO_3^{2-}. TeO_3^- is a strong reducing agent ($E_{o(red)}$ = −0.40 V), which appears to reduce O_2, as well as a strong oxidant ($E_{o(ox)}$ = 1.74 V), oxidizing CO_3^{2-} to CO_3^-.

Introduction

Oxoradicals of the group six elements sulfur, selenium, and tellurium in the oxidation state V may be formed in aqueous solution.[1–6] The only S(V) radical observed is SO_3^-; selenium similarly forms SeO_3^- and, in strongly alkaline solution also, $HSeO_4^{2-}$. Whereas the S(V) and Se(V) radicals have been characterized in detail, little is known about the properties of the corresponding oxoradicals of tellurium. However, it has been shown previously that Te(V), like S(V) and Se(V), is amenable to study in aqueous solution by the pulse radiolysis technique.[7–9] Here Te(V) species may be formed by reduction of telluric acid (H_6TeO_6) and the tellurates ($H_5TeO_6^-$, $H_4TeO_6^{2-}$) with the hydrated electron, e_{aq}^-, as well as by oxidation of hydrogen tellurite ($HTeO_3^-$) and tellurite (TeO_3^{2-}) with OH or O^-. A transient absorbance detected in an O_2-containing tellurite solution after irradiation was assigned to TeO_3^{-}[9], a species similar to SO_3^- [1–5] and SeO_3^-.[6,10] This assignment was substantiated by the detection of TeO_3^- in tellurite crystals irradiated with X-rays.[11] TeO_3^- has in the solid matrix the same symmetry (C_{3v}) as TeO_3^{2-}.[12] Also reactions of e_{aq}^- with telluric acid and tellurate have been studied, but no transient absorbance was assigned to Te(V) species.[7,8]

Since not only SeO_3^- but also $HSeO_4^{2-}$ are observed by pulse radiolysis of aqueous selenite and selenate solutions[6] a more comprehensive pulse radiolysis study of aqueous tellurite and tellurate may be expected similarly to reveal the formation of tellurium(V) species other than TeO_3^-. In the present study, we have measured the spectra and kinetics of the transient absorbances that arise in aqueous solution by the reaction of OH and O^- with tellurous acid, and of those that arise by the reaction of e_{aq}^- with telluric acid. On the basis of these measurements we assign the absorbances to four Te(V) species of definite composition, and their evolution in time to reactions among these species. We have determined rate constants for the reactions and constants for the observed equilibria involving Te(V) species, and estimated the standard free energy of formation of these species. Moreover, we have measured the kinetics of the reactions of the Te(V) species with molecular oxygen and with hydrogen carbonate and carbonate. The properties of Te(V) oxoradicals are compared to those of the corresponding S(V) and Se(V) oxoradicals.

Experimental Section

Pulse radiolysis was made at ambient temperature (21 ± 1 °C) with the HCR linac at Risø delivering 10 MeV in single square pulses. The pulse length was varied between 0.1 and 1 μs. The dose, ranging from 2.5 to 20 Gy, was measured with the ferrocyanide dosimeter[13] taking the extinction coefficient of ferricyanide at 420 nm equal to 1000 cm^{-1} M^{-1} and the G-value (molecules/100 eV) for formation of ferricyanide equal to 5.9. Yields of products were calculated from the measured dose using published G-values[14] corrected for spur reactions.[15] The experimental setup for irradiation and for kinetic spectroscopy measurements were as previously described.[6] Chemicals were reagent grade or of higher purity. Solutions were prepared with triply distilled water. Nitrous oxide, N48 (purity 99.998%), was ALPHAGAZ. Argon, oxygen, and nitrogen, all N40 (purity 99.99%), were supplied by Dansk Ilt og Brint.

Solutions were purged of oxygen by bubbling-through with Ar or N_2O at 0.1 MPa. In studies of reactions of e_{aq}^-, Ar was

---

* Author to whom correspondence should be addressed.

† Present address: Møllegaarden, Obstrupvej 12 M, DK-8320 Maarslet, Denmark.

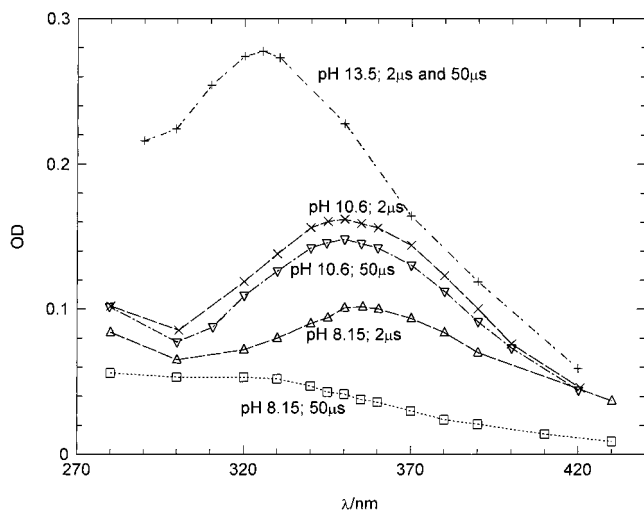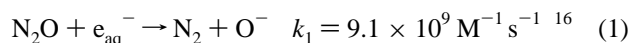‡ Strandhøjen 5, Himmelev, DK-4000 Roskilde, Denmark.

Figure 1. Transient absorption spectra measured 2 μs and 50 μs after irradiation (dose 19.8 Gy) of 2 $\times$ 10^{-4} M tellurite/hydrogen tellurite solutions at pH 8.15, 10.6, and 13.5.

Figure 2. Absorbance at 300 and 380 nm as a function of time measured in 2 $\times$ 10^{-4} M hydrogen tellurite at pH 8.15 after irradiation (dose 19.8 Gy).

Figure 3. Absorbance at 380 nm as a function of time measured in 2 $\times$ 10^{-4} M tellurite/hydrogen tellurite solutions at various pH values after irradiation (dose19.8 Gy). The smooth curves are simulations calculated with the Gepasi package[21−23] (see text).

used. N$_2$O was used when interference from reactions of e$_{aq}^-$ were to be avoided. N$_2$O converts e$_{aq}^-$ into O$^-$ in a fast reaction,

$$N_2O + e_{aq}^- \rightarrow N_2 + O^- \quad k_1 = 9.1 \times 10^9 \, M^{-1} s^{-1} \quad {}^{16} \quad (1)$$

pH was adjusted by addition of sodium hydroxide and perchloric acid and was, for pH < 12, measured with a pH-meter (Radiometer pH M 64). For pH > 12, pH was taken equal to 14 + log[NaOH]. The pK-values for the dissociations of tellurous and telluric acid were determined by pH-metric titration of 10^{-3} M sodium tellurite and telluric acid with perchloric acid and sodium hydroxide, respectively, using a Radiometer titrator TTT 60 fitted with a Radiometer autoburette ABU (volume 0.25 mL). For H$_2$TeO$_3$ we found pK_1 = 6.3 and pK_2 = 9.6, and for H$_6$TeO$_6$ pK_1 = 7.8 and pK_2 = 11.0, in agreement with recently recommended values.[17]

Simulation of kinetic data was performed using the computer package "Gepasi" equipped with the optimization module Multistart (Levenberg−Marquardt) Version 1.00.[18−20]

Results and Discussion

Reaction of H$_2$TeO$_3$ and HTeO$_3^-$ with OH, and Reactions of TeO$_3^{2-}$ with OH and O$^-$. The measurements were made with 10^{-4}−10^{-2} M solutions prepared from sodium tellurite at pH ranging from 6.6 to 13.5. Measurements at pH < 6 proved unreliable since such solutions became turbid on standing. Upon irradiation of N$_2$O-saturated tellurous solutions, a transient absorbance was observed to grow-in at λ < 430 nm in a pseudo first-order reaction with a rate constant proportional to the concentration of tellurous acid. We ascribe the transient absorbance to formation of Te(V) species by reactions of OH and O$^-$. (Absorbance changes owing to removal of Te(IV) by the irradiation were neglected throughout.) The spectrum and the time evolution of the transient absorbance depend on pH. Figures 1, 2, and 3, illustrate the absorbance changes observed after irradiation of 2 $\times$ 10^{-4} M Te(IV) solutions with a dose of 19.8 Gy. Figure 1 shows the spectrum of the transient absorbance measured 2 μs and 50 μs after the irradiation at pH 8.15, 10.6, and pH 13.5. The three spectra are clearly distinct initially (at 2 μs), and they evolve differently in time. At pH 13.5, no time evolution is detected. At pH 10.6, the absorbance decreases only slightly with time while the spectrum is unchanged. In contrast,
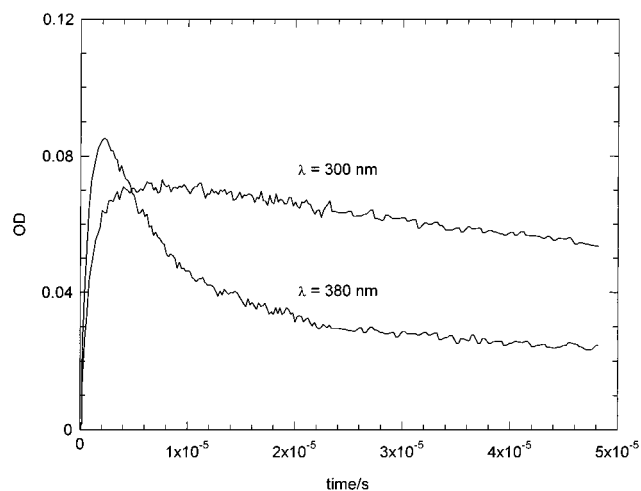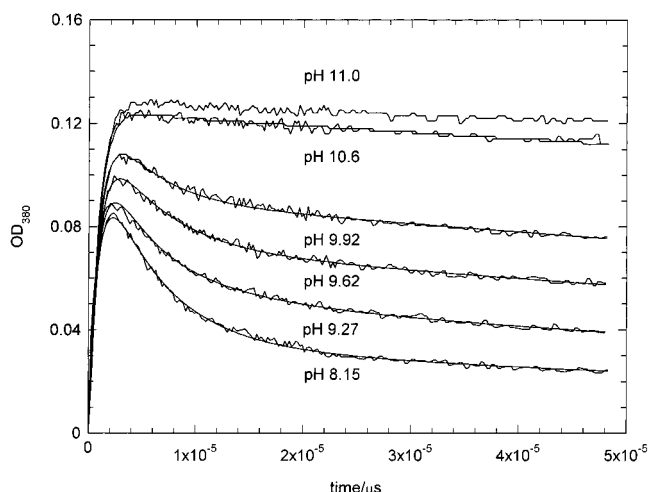
the spectrum recorded at pH 8.15 2 μs after the irradiation is very different from that recorded after 50 μs, the initial maximum at 355 nm giving way to a shoulder at ∼340 nm. Figure 2, showing the absorbance change at 300 and 380 nm during the first 50 μs after the irradiation, illustrates this process. After a fast increase at both wavelengths owing to the reaction of HTeO$_3^-$ with OH, the absorbance at 300 nm further increases for the next 10 μs, while the absorbance at 380 nm suffers a decrease on the same time scale. Figures 1 and 2 suggest the formation of four species, of which three, displaying a maximum absorbance at 325−350 nm, are Te(V) species formed in primary reactions of OH and O$^-$ with Te(IV), and the fourth, associated with the shoulder at 345 nm and also assumed to be a Te(V) species, is formed from the primary Te(V) species that predominates at pH 8.15. Further measurements have shown that the absorbance change associated with the formation of the fourth species is independent of pH in the range from 6.6 (the lowest pH used) to 8.5 and is of first order with a rate constant that increases linearly with the total concentration of Te(IV).

Figure 3 shows the pH-dependence of the transient absorbance at 380 nm. The absorbance increases with increasing pH and

Tellurium(V). A Pulse Radiolysis Study

J. Phys. Chem. A, Vol. 105, No. 27, 2001 **6639**

the fast decay associated with the formation of the fourth (secondary) Te(V) species decreases steadily, indicating the appearance and growing importance of a new Te(V) species that is stable on the 10 μs time scale. Between pH 11 and 12 no further change of absorbance with pH was observed, suggesting that one Te(V) species predominates in this pH interval. At pH > 12 the absorbance increases further with increasing pH, while the maximum absorbance shifts toward shorter wavelengths, indicating the formation of yet another Te(V) species. The eventual decay of the transient absorbance is a second-order process with a rate constant that decreases with increasing pH.

The spectra of the primary Te(V) species are alike, in the sense that they all display a maximum in the region from 325 nm to 360 nm, whereas the secondary formed species has a quite different spectrum. We take this to suggest that the three primary Te(V) species have the same coordination at the tellurium atom and that the formation of the secondary species involves a change of coordination at the tellurium atom.

A consistent interpretation of these observations may be achieved by assigning the three primary transient spectra to the four-coordinated Te(V) oxoanions $H_2TeO_4^-$, $HTeO_4^{2-}$, and TeO_4^{3-}. In neutral and slightly alkaline solutions $H_2TeO_4^-$ is formed by addition of OH to H_2TeO_3 and $HTeO_3^-$,

$$H_2TeO_3 + OH \rightarrow H_2TeO_4^- + H^+ \quad k_2 \quad (2)$$

$$HTeO_3^- + OH \rightarrow H_2TeO_4^- \quad k_3 \quad (3)$$

We note that the same Te(V) species appears to be formed at pH 6.6 and at pH 8.5, despite the fact that at pH 6.6 around 30% of Te(IV) is present as H_2TeO_3 whereas $HTeO_3^-$ predominates at pH 8.15. Hence, one might expect to observe the formation of H_3TeO_4 as well as of $H_2TeO_4^-$ at pH 6.6. However, using Pauling's rule for the strength of oxoacids,[21] which suggests a dissociation constant of the order of 10^{-3} for the acid H_3TeO_4, and the commonly accepted estimate ($10^{10}-10^{11}$ M^{-1} s^{-1}) for the rate constant of a reaction such as that of H^+ with $H_2TeO_4^-$,[22] we find a rate constant for the protolysis of the order of 10^7-10^8 s^{-1}, in keeping with the absence of a transient assignable to H_3TeO_4.

With increasing pH, the composition of the Te(IV) substrate shifts toward TeO_3^{2-}; $HTeO_4^{2-}$ formed by

$$TeO_3^{2-} + OH \rightarrow HTeO_4^{2-} \quad k_4 \quad (4)$$

therefore gains importance and dominates at 11 < pH < 12.

At pH > 12, OH gives way to O^- and TeO_4^{3-} formed by addition of O^- to TeO_3^{2-}

$$TeO_3^{2-} + O^- \rightarrow TeO_4^{3-} \quad k_5 \quad (5)$$
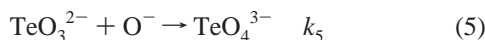
becomes important.

We assign the secondary, transient spectrum that dominates after 50 μs at low pH to TeO_3^-. Hence we ascribe the spectral evolution seen at 8.15 < pH < 10 (Figure 1) to a transformation of $H_2TeO_4^-$ into TeO_3^-, occurring either by a dehydration

$$H_2TeO_4^- \rightarrow TeO_3^- + H_2O \quad k_6 \quad (6)$$

catalyzed equally by H_2TeO_3 and $HTeO_3^-$

$$H_2TeO_4^- + HTeO_3^-/H_2TeO_3 \rightarrow$$
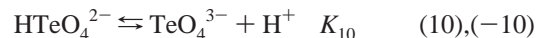$$TeO_3^- + H_2O + HTeO_3^-/H_2TeO_3 \quad k_{6a} \quad (6a)$$

or by reaction of $H_2TeO_4^-$ with TeO_3^{2-}

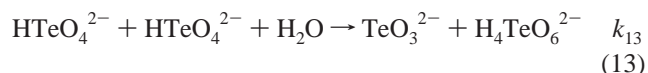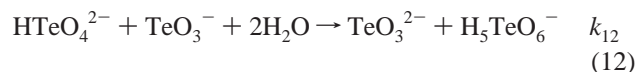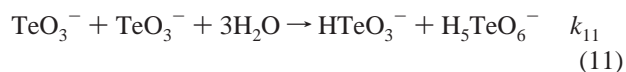$$H_2TeO_4^- + TeO_3^{2-} \rightarrow HTeO_3^- + HTeO_4^{2-} \quad k_7 \quad (7)$$

We point out that a dehydration taking place by reactions similar to reactions 6 and 6a were previously observed by pulse radiolysis of solutions of arsenite.[23] Here the As(IV) species $As(OH)_4$ and $As(OH)_3O^-$ formed by addition of OH to H_3AsO_3 and $H_2AsO_3^-$ dehydrate subsequently to yield H_2AsO_3 and $HAsO_3^-$, respectively.

The Te(V) species participate in the protolytic equilibria

$$TeO_3^- + H_2O \leftrightarrows H_2TeO_4^- \leftrightarrows HTeO_4^{2-} + H^+ \quad K_{8,9}$$
$$(8),(-8),(9),(-9)$$

$$HTeO_4^{2-} \leftrightarrows TeO_4^{3-} + H^+ \quad K_{10} \quad (10),(-10)$$
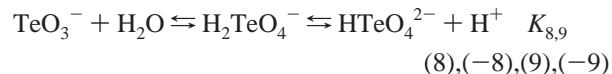
The second-order decay of absorbance observed at pH < 12 is ascribed to the reactions

$$TeO_3^- + TeO_3^- + 3H_2O \rightarrow HTeO_3^- + H_5TeO_6^- \quad k_{11} \quad (11)$$

$$HTeO_4^{2-} + TeO_3^- + 2H_2O \rightarrow TeO_3^{2-} + H_5TeO_6^- \quad k_{12} \quad (12)$$

$$HTeO_4^{2-} + HTeO_4^{2-} + H_2O \rightarrow TeO_3^{2-} + H_4TeO_6^{2-} \quad k_{13} \quad (13)$$

An additional reaction is suggested to be important at pH > 12

$$HTeO_4^{2-} + TeO_4^{3-} + 2H_2O \rightarrow$$
$$TeO_3^{2-} + H_4TeO_6^{2-} + OH^- \quad k_{14} \quad (14)$$
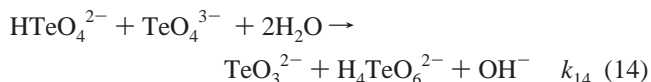
Reaction of e_{aq}^- with H_6TeO_6, $H_5TeO_6^-$, and $H_4TeO_6^{2-}$. Transient absorbances in O_2-free $10^{-3}-10^{-2}$ M telluric acid solutions saturated with Ar were measured in the pH-range from 5.5 to 13.5. Here the formation of Te(V) species in the reactions of e_{aq}^- with H_6TeO_6, $H_5TeO_6^-$, and $H_4TeO_6^{2-}$ can be studied. Interfering reactions of OH and O^- with telluric acid and tellurate may conceivably occur in such solutions. However, no transient absorption was observed if e_{aq}^- was quenched by N_2O (reaction 1), suggesting that reactions of OH with telluric acid and of O^- and OH with tellurate are slow compared to other reactions that remove O^- and OH. (This observation also indicates that reactions of H atoms with Te(VI) can be neglected).

The transient absorption spectra that arise in tellurate solutions at pH > 11 are similar to those observed at the same pH in N_2O-saturated tellurite solutions and assigned above to $HTeO_4^{2-}$ and TeO_4^{3-}. This indicates the occurrence of the reactions

$$H_5TeO_6^- + e_{aq}^- \rightarrow HTeO_4^{2-} + 2H_2O \quad (4a)$$

and

$$H_4TeO_6^{2-} + e_{aq}^- \rightarrow TeO_4^{3-} + 2H_2O \quad (5a)$$

In the pH range 11 < pH < 12, where the Te(V) species $HTeO_4^{2-}$ dominates, the absorbance decays somewhat faster than in tellurite solutions. The process seems to be of mixed first and second order. In solutions at pH > 12, the absorbance decays in a first-order process rather than the second-order process observed in tellurite solutions. However, in an Ar-

TABLE 1: Summary of Reactions and Constants

reaction/equilibrium	rate constant/M^{-1} s^{-1}; pK-values	ionic strength/M
$N_2O + e_{aq}^- \rightarrow N_2 + O^-$	$k_1 = 9.1 \times 10^{9\ a}$	
$H_2TeO_3 + OH \rightarrow H_2TeO_4^- + H^+$	$k_2 = (6 \times 10^9) - (8 \times 10^9)\ ^b$	$< 10^{-3}$
$HTeO_3^- + OH \rightarrow H_2TeO_4^-$	$k_3 = (6.2 \pm 0.6) \times 10^{9\ c}$	$< 10^{-3}$
$TeO_3^{2-} + OH \leftrightarrows HTeO_4^{2-}$	$k_4 = (4.8 \pm 0.5)b \times 10^9;^c\ k_{-4} = (1.3 \pm 0.4) \times 10^{3\ c,d}$	$< 10^{-3}$; $10^{-2}-0.3$
$TeO_3^{2-} + O^- \leftrightarrows TeO_4^{3-}$	$k_5 = (1.0 \pm 0.10) \times 10^9;^c\ k_{-5} = 3.7 \pm 0.4 \times 10^{3\ c,d}$	0.1; $10^{-2}-0.3$
$H_2TeO_4^- \rightarrow TeO_3^- + H_2O$	$k_6 \sim 10^{4\ b,c,d}$	$< 5 \times 10^{-3}$
$H_2TeO_4^- + HTeO_3^- \rightarrow TeO_3^- + H_2O + HTeO_3^-$	$k_{6a} = (8.6 \pm 0.8) \times 10^{8\ c}$	$< 5 \times 10^{-3}$
$H_2TeO_4^- + TeO_3^{2-} \rightarrow HTeO_4^{2-} + HTeO_3^-$	$k_7 \sim 10^{8\ b}$	$< 10^{-3}$
$TeO_3^- + H_2O \leftrightarrows H_2TeO_4^- \leftrightarrows HTeO_4^{2-} + H^+$	p$K_{8,9} = 9.96 \pm 0.15\ ^c$	$10^{-2} - 3 \times 10^{-2}$
$HTeO_4^{2-} \leftrightarrows TeO_4^{3-} + H^+$	p$K_{10} = 13.2 \pm 0.2$	$10^{-2} - 0.3$
$TeO_3^- + TeO_3^- + 3H_2O \rightarrow HTeO_3^- + H_5TeO_6^-$	$k_{11} = (4.7 \pm 0.8) \times 10^{8\ c}$	$< 10^{-2}$
$HTeO_4^{2-} + TeO_3^- + 2H_2O \rightarrow TeO_3^{2-} + H_5TeO_6^-$	$k_{12} = (1.1 \pm 0.2) \times 10^{9\ c}$	$< 10^{-2}$
$HTeO_4^{2-} + HTeO_4^{2-} + H_2O \rightarrow TeO_3^{2-} + H_4TeO_6^{2-}$	$k_{13} = (1.2 \pm 0.4) \times 10^{7\ c}$	$< 10^{-2}$
$H_6TeO_6 + e_{aq}^- \rightarrow TeO_3^- + 3H_2O$	$k_{15} = 3.2 \times 10^{10\ e}$	
$OH + OH \rightarrow H_2O_2$	$k_{17} = 5.5 \times 10^{10\ a}$	
$OH + H \rightarrow H_2O$	$k_{18} = 7 \times 10^{9\ a}$	
$TeO_3^- + O_2 \rightarrow TeO_5^-$	$k_{33} = (6.8 \pm 0.7) \times 10^{8\ c}$	$< 10^{-3}$
$HTeO_4^{2-} + O_2 \rightarrow TeO_5^- + OH^-$	$k_{34} = (2.9 \pm 0.17) \times 10^{8\ c}$	$< 10^{-2}$
$TeO_4^{3-} + O_2 + H_2O \rightarrow TeO_5^- + 2OH^-$	$k_{35} = (2.5 \pm 0.3) \times 10^{8\ c}$	0.2
$HCO_3^- + TeO_3^- \rightarrow CO_3^- + HTeO_3^-$	$k_{37} = (1.6 \pm 0.5) \times 10^{6\ c}$	$2 \times 10^{-2} - 0.2$
$CO_3^{2-} + TeO_3^- \rightarrow CO_3^- + TeO_3^{2-}$	$k_{38} = (1.7 \pm 0.5) \times 10^{7\ c}$	$2 \times 10^{-2} - 0.2$

^{a} Ref 16. ^{b} Value estimated. ^{c} This work. ^{d} s^{-1}. ^{e} Ref 7.

saturated solution containing both tellurite and tellurate in equal concentrations, where OH and O^- react with tellurite and e_{aq}^- reacts with tellurate, the decay of absorbance was of second order with a rate constant similar to that measured in N_2O-saturated tellurite solutions at the same pH. These observations suggest that $HTeO_4^{2-}$ and TeO_4^{3-} may disappear by the reverse of reactions 4 and 5

$$HTeO_4^{2-} \rightarrow TeO_3^{2-} + OH \quad k_{-4} \qquad (-4)$$

$$TeO_4^{3-} \rightarrow TeO_3^{2-} + O^- \quad k_{-5} \qquad (-5)$$
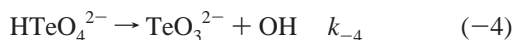
as well as by the reactions 13 and 14. The reactions -4 and -5 parallel the thermal split-off of O^- or OH from the electron adducts of selenate,[6] periodate,[24] and perxenate.[25]

At pH < 11, the transient absorption spectrum is similar to that observed in tellurite solutions after the transient ascribed to $H_2TeO_4^-$ has decayed. Moreover, the absorbance decays without change of spectrum in a second-order process that matches the decay of TeO_3^-.

These observations indicate that TeO_3^- is formed directly by reaction of e_{aq}^- with H_6TeO_6

$$H_6TeO_6 + e_{aq}^- \rightarrow TeO_3^- + 3H_2O \quad k_{15} \qquad (15)$$
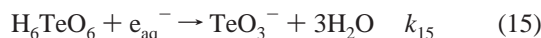
rather than via $H_2TeO_4^-$ as is the case in the reaction of OH with $HTeO_3^-$.

The reactions and equilibria discussed above are summarized in Table 1.

Determination of the Spectra of TeO_3^-, $H_2TeO_4^-$, $HTeO_4^{2-}$, and TeO_4^{3-}. The spectra of TeO_3^-, $H_2TeO_4^-$, $HTeO_4^{2-}$, and TeO_4^{3-}, represented as the extinction coefficients versus wavelength, $\epsilon_{TeO_3^-}(\lambda)$, $\epsilon_{H_2TeO_4^-}(\lambda)$, $\epsilon_{HTeO_4^{2-}}(\lambda)$, and $\epsilon_{TeO_4^{3-}}(\lambda)$, are shown in Figure 4. $\epsilon_{TeO_3^-}(\lambda)$, $\epsilon_{HTeO_4^{2-}}(\lambda)$, and $\epsilon_{TeO_4^{3-}}(\lambda)$, were obtained from transient absorbances measured in 2×10^{-3} M telluric acid 2 μs after the irradiation at pH 8, 11.4, and 13.48, respectively. At that time the primary reaction of e_{aq}^- as well as the subsequent protolytic reactions are completed whereas, on the other hand, the slow second-order decay of the absorbance may be neglected.
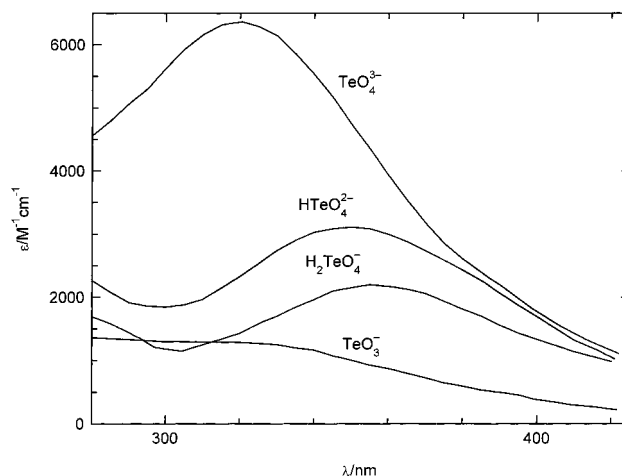

Figure 4. Spectra of TeO_3^-, $H_2TeO_4^-$, $HTeO_4^{2-}$, and TeO_4^{3-} calculated from measurements (see text).

Owing its large base strength, TeO_4^{3-} cannot be made the predominant Te(V) solute. $\epsilon_{TeO_4^{3-}}(\lambda)$ was obtained from eq 16

$$\epsilon_{TeO_4^{3-}}(\lambda) = (\epsilon(\lambda) - \epsilon_{HTeO_4^{2-}}(\lambda)\,(1 - x_{TeO_4^{3-}}))/x_{TeO_4^{3-}} \quad (16)$$

where $\epsilon(\lambda)$ is the spectrum of the equilibrium mixture of TeO_4^{3-} and $HTeO_4^{2-}$ in 0.3 M NaOH, and $x_{TeO_4^{3-}}$ is the fraction of Te(V) present as TeO_4^{3-}, found to be 0.63 in 0.3 M NaOH (see eq 25 below).

The overlap of reactions 2 and 3 with reactions 6 and 6a precludes a direct determination of the spectrum of $H_2TeO_4^-$. $\epsilon_{H_2TeO_4^-}(\lambda)$ shown in Figure 4 was calculated from absorbances measured 2 μs after the irradiation of a tellurite solution at pH 8 (where Te(V) species other than TeO_3^- and $H_2TeO_4^-$ may be neglected) and the concentrations at that time of $H_2TeO_4^-$ and TeO_3^-. These concentrations were obtained as a function of time from a simulation of the absorbance at 350 nm during the first 5 μs after the irradiation. The simulation was based on the reactions 3, 6 and 6a, accounting for the formation of $H_2TeO_4^-$ and its transformation into TeO_3^-, respectively,

Tellurium(V). A Pulse Radiolysis Study

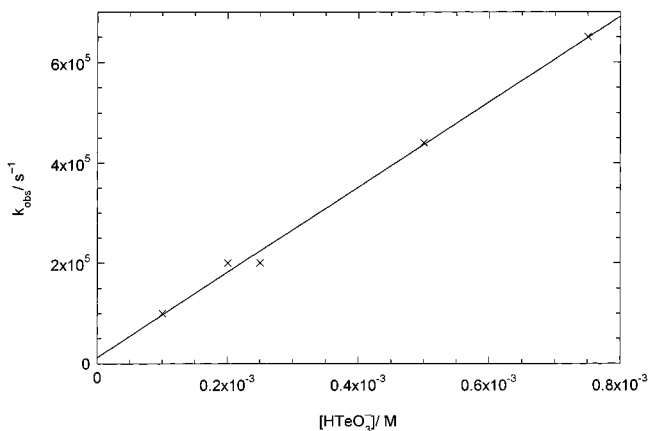*J. Phys. Chem. A, Vol. 105, No. 27, 2001* **6641**

Figure 5. Dehydration of $H_2TeO_4^-$. The pseudo first-order rate constant k_{obs} at pH 8 for the dehydration of $H_2TeO_4^-$ (reactions 6 and 6a) plotted against the concentration of $HTeO_3^-$. $\times$ represents experimental points; the straight line is a linear least-squares fit to the experimental points. The slope is k_{6a} (Table 1).

supplemented by the competing removal of OH by reactions 17 and 18

$$OH + OH \rightarrow H_2O_2 \tag{17}$$

$$H + OH \rightarrow H_2O \tag{18}$$
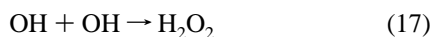
The value of $\epsilon_{TeO_3^-}$ at 350 nm and the values of the rate constants k_3, k_6 and k_{6a} used in the simulation were as determined (Table 1). The rate constants of reactions 17 and 18 were taken to be 5.5×10^9 M^{-1} s^{-1} [16] and 7×10^9 M^{-1} s^{-1},[16] respectively. Fitting the calculated absorbance to the measured by adjusting the value of $\epsilon_{H_2TeO_4^-}$ at 350 nm, we then obtained the concentrations of $H_2TeO_4^-$ and TeO_3^- 2 μs after the irradiation. With these concentrations and $\epsilon_{TeO_3^-}(\lambda)$, we obtained $\epsilon_{H_2TeO_4^-}(\lambda)$ shown in Figure 4 from the measured absorbance.

Determination of Rate Constants for Reactions of $H_2TeO_4^-$, TeO_3^-, $HTeO_4^{2-}$, and TeO_4^{3-}. Rate constants determined below are shown in Table 1. Throughout the analysis we neglect possible reactions of hydrogen tellurite and tellurite with the hydrogen atom formed in the primary radiolytic process.

Recalling that the observed kinetics of absorbance change was independent of pH in the region from 6 to 8.5, we may assume that the rate constants k_2 and k_3 for the reactions of OH with H_2TeO_3 and $HTeO_3^-$ are similar. k_3 and the rate constants for the reactions of OH and O$^-$ with TeO_3^{2-}, k_4 and k_5, were determined from the rate of growing-in of the absorbance at 350 nm after irradiation of 10^{-4} M hydrogen tellurite and tellurite solutions with 2.5 Gy (Table 1). The values of k_3 and k_5 were determined from the rate observed in solutions at pH 8 and at pH 13.3, respectively. Then, k_4 was determined from the relation

$$k_{19} = k_4 \times x_{OH} + k_5 \times (1 - x_{OH}) \tag{19}$$

where $k_{19} = 4.4 \times 10^9$ M^{-1} s^{-1} is the rate constant for formation of tellurium(V) at pH 10.9 and x_{OH} is given by $x_{OH} = (1 + K_{OH} \times 10^{pH})^{-1}$, under the assumption that the equilibrium between OH and O$^-$ is maintained during the reaction ($K_{OH} = 10^{-11.9}$).[16]

The rate constants k_6 and k_{6a} for the uncatalyzed and the catalyzed dehydration of $H_2TeO_4^-$ were obtained from measurements of the rate constant k_{obs} for the decrease of absorbance at 350 nm in solutions at pH 8 containing $HTeO_3^-$ in varying concentration. Figure 5 shows a plot of k_{obs} against $[HTeO_3^-]$.

k_6 and k_{6a} shown in Table 1 were obtained from a fit of a linear function to the plot, k_6 as the constant term, and k_{6a} as the coefficient to $[HTeO_3^-]$. We note that the data do not allow an accurate determination of k_6. We find k_6 to be around 10^4 s^{-1}, which is the same order of magnitude as found for the uncatalyzed dehydration of the As(IV) species As(OH)$_3$O$^-$.[23]

Reaction 7 between $H_2TeO_4^-$ and TeO_3^{2-} was not observed directly. A value of $\sim 10^8$ M^{-1} s^{-1} was estimated for the rate constant, k_7.

The rate constants k_{11}, k_{12}, and k_{13} for the reactions 11$-$13, by which TeO_3^- and $HTeO_4^{2-}$ disappear, were determined from k_{22}, the second-order rate constant for the decay of the absorbance OD(t) at 350 nm measured at pH values between 8.15 and 11.76. Since in the actual experiments pH remains constant and equilibrium between TeO_3^- and $HTeO_4^{2-}$ is maintained during the decay, the fraction $x_{TeO_3^-}$ of the total concentration $c(t)$ of Te(V) that is present as TeO_3^- remains constant. Consequently, the integrated rate equation for the simultaneous disappearance of TeO_3^- and $HTeO_4^{2-}$ may be expressed by

$$c(t)^{-1} - c(t=0)^{-1} = (2k_{11} \times x^2_{TeO_3^-} + k_{12} \times$$
$$x_{TeO_3^-} (1 - x_{TeO_3^-}) + 2k_{13} \times (1 - x_{TeO_3^-})^2) \times t \tag{20}$$

where $x_{TeO_3^-} = (1 + K_{8,9} \times 10^{pH})^{-1}$; ($K_{8,9} = 1.1 \times 10^{-10}$, see below).

The integrated rate equation for disappearance of the absorbance may be expressed by

$$OD(t)^{-1} - OD(t=0)^{-1} = k_{22} \times t = (c(t)^{-1} - c(t=0)^{-1})/$$
$$(l \times \epsilon_{TeO_3^-} \times x_{TeO_3^-} + l \times \epsilon_{HTeO_4^{2-}} \times (1 - x_{TeO_3^-})) \tag{21}$$

where l is the length of the optical cell (5.5 cm).

From eqs 20 and 21 we find

$$k_{22} = (2k_{11} \times x^2_{TeO_3^-} + k_{12} \times x_{TeO_3^-} (1 - x_{TeO_3^-}) + 2k_{13} \times$$
$$(1 - x_{TeO_3^-})^2)/(l \times \epsilon_{TeO_3^-} \times x_{TeO_3^-} + l \times \epsilon_{HTeO_4^{2-}} \times$$
$$(1 - x_{TeO_3^-})) \tag{22}$$

Figure 6 shows a plot of $k_{22} \times (l \times \epsilon_{TeO_3^-} \times x_{TeO_3^-} + l \times \epsilon_{HTeO_4^{2-}} \times (1 - x_{TeO_3^-}))$ against $x_{TeO_3^-}$ together with the least-squares fit of a quadratic function to the experimental points. By equating coefficients to like powers of $x_{TeO_3^-}$ in eq 20 and in the quadratic function, we find the values for k_{11}, k_{12}, and k_{13}, shown in Table 1.

The rate constants k_{-4} and k_{-5} were determined from the first-order rate constant, k_{23}, for the decay of absorbance at 325 nm, measured at pH varying between 12.19 and 13.48. k_{23} may be expressed by

$$k_{23} = k_{-5} \times x_{TeO_4^{3-}} + k_{-4} \times (1 - x_{TeO_4^{3-}}) \tag{23}$$

where $x_{TeO_4^{3-}} = K_{10} \times 10^{pH}/(1 + K_{10} \times 10^{pH})$ is the fraction of the total Te(V) concentration that is present as TeO_4^{3-} in equilibrium with $HTeO_4^{2-}$. Figure 7 shows a plot of k_{23} against $x_{TeO_4^{3-}}$. k_{-4} and k_{-5} were found by fitting a linear function to the experimental points (Table 1).

Test of the Mechanism. The rate constants of the mechanism proposed above were determined under the assumption that overlap among the individual reactions could be neglected. However, a test performed without this assumption by simulating the time evolution of the absorbance measured at 380 nm in N$_2$O-saturated 2×10^{-4} M tellurite solutions at pH 8.15,
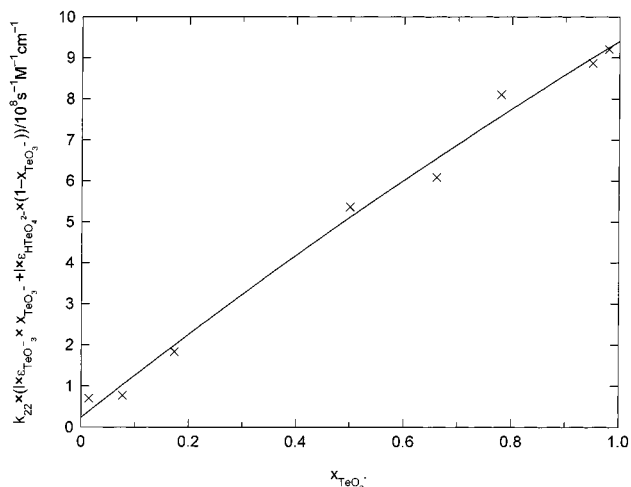
Figure 6. Determination of the second-order rate constants, k_{11}, k_{12}, and k_{13}, for the disappearance of TeO_3^- and $HTeO_4^{2-}$. $k_{22} \times (1 \times \epsilon_{TeO_3^-} \times x_{TeO_3^-} + 1 \times \epsilon_{HTeO_4^{2-}} \times (1 - x_{TeO_3^-}))$ is plotted against $x_{TeO_3^-}$. k_{22} is the rate constant of the second-order decay of absorbance at 350 nm (see text). $x_{TeO_3^-}$ is the fraction of TeO_3^- present in the equilibrium mixture of TeO_3^- and $HTeO_4^{2-}$. Concentration of tellurite/hydrogen tellurite: 2×10^{-4} M; dose 19.8 Gy; pH varies between 8 and 11. $\times$ represents experimental points, the full line represents a least-squares fit of a quadratic function of $x_{TeO_3^-}$ to the experimental points.
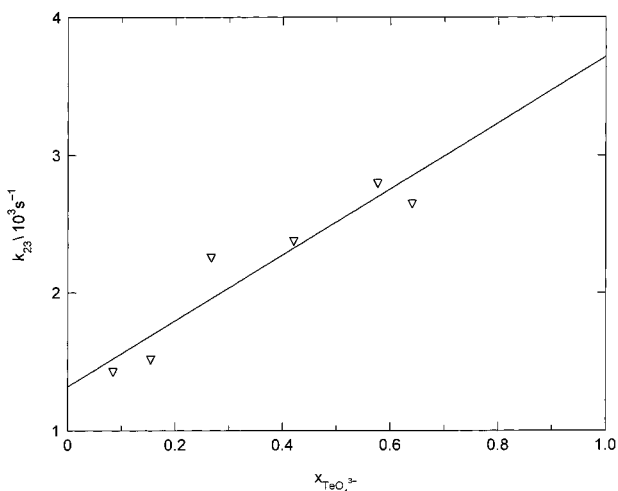
Figure 7. Determination of the rate constants k_{-4} and k_{-5} for the dissociation of $HTeO_4^{2-}$ into TeO_3^{2-} and OH and the dissociation of TeO_4^{3-} into TeO_3^{2-} and O^-, respectively. $k_{23} = k_{-5} \times \epsilon_{TeO_4^{3-}} \times x_{TeO_4^{3-}} + k_{-4} \times \epsilon_{HTeO_4^{2-}} \times (1 - x_{TeO_4^{3-}})$ is plotted against $x_{TeO_4^{3-}}$. $x_{TeO_4^{3-}}$ is the fraction of TeO_4^{3-} present in the equilibrium mixture of TeO_4^{3-} and $HTeO_4^{2-}$. k_{23} is the first-order rate constant for the decay of absorbance at 325 nm. The straight line shows of a linear least-squares fit to the experimental points ($\times$).

9.27, 9.62, 9.92, and 10.6, showed that the mechanism is consistent with this set of data (Figure 3). At pH 8.15, where the species $H_2TeO_4^-$ and TeO_3^- dominate, the important reactions of the mechanism are 3, 6, 6a, 11, 17, and 18. Here the calculated absorbance was fitted to the measured absorbance by adjusting the dose, allowing it to vary within $\pm 4\%$ of the nominal value, whereas the rate constants had the values given in Table 1, and the extinction coefficients of $H_2TeO_4^-$ and TeO_3^- at 380 nm were those shown in Figure 4.

At pH 9.27, 9.62, 9.92, and 10.6, the additional reactions 4, 7, 12, 13, as well as
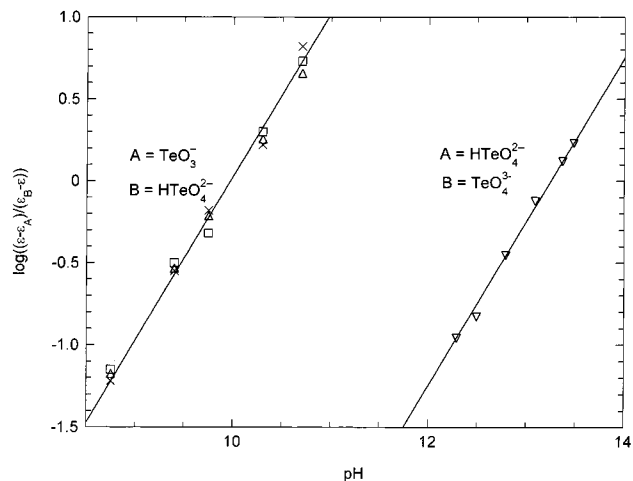
$$TeO_3^- + B^- + H_2O \rightleftharpoons HTeO_4^{2-} + HB \quad (24),(-24)$$

Figure 8. $pK_{8,9}$, the apparent acid dissociation constant of TeO_3^-, and pK_{10}, the acid dissociation constant of $HTeO_4^{2-}$, determined from plots of the quantity $\log(\epsilon - \epsilon_A)/(\epsilon_B - \epsilon)$ against pH. In the left curve A and B stand for TeO_3^- and $HTeO_4^{2-}$, and in the right curve for $HTeO_4^{2-}$ and TeO_4^{3-}, respectively. Δ, $\square$, $\times$, and ∇, are experimental points, Δ measured at 350 nm, $\square$ at 400 nm, $\times$ at 425 nm, and ∇ at 325 nm. Straight lines are linear least-squares fits to the experimental points.

where ($B^- = TeO_3^{2-}$ and OH^-), involving the species $HTeO_4^{2-}$, become important. Here the test was performed by fitting calculated absorbances to the measured absorbances by adjusting three parameters: the dose, again only within $\pm 4\%$ of the nominal value, and the pseudo first-order rate constants $k_{24}[B^-]$ and $k_{-24}[HB]$. The rate constants of reactions 3, 4, 6, 7, 11, 12, 13, 17, and 18, were taken from Table 1 and the extinction coefficients of $H_2TeO_4^-$, TeO_3^-, and $HTeO_4^{2-}$ were as measured (Figure 4).

From pH and the corresponding values obtained for $k_{24}[B^-]$ and $k_{-24}[HB]$ in the four solutions we find

$$pK = pH + \log(k_{-24}[HB]/k_{24}[B^-]) = 9.94 \pm 0.13 \quad (25)$$

in agreement with the value for pK ($pK_{8,9}$) = 9.96 $\pm$ 0.15 determined by the equilibrium measurements described below and therefore indicating the consistency of the mechanism for these four solutions also.

Equilibrium Constants, Standard Gibbs Energy of Formation, and Standard Electrode Potentials of TeO_3^-, $H_2TeO_4^-$, $HTeO_4^{2-}$, and TeO_4^{3-}. The values of pK for the apparent acid dissociation of TeO_3^-, $pK_{8,9}$ = 9.96 $\pm$ 0.15, and for the acid dissociation of $HTeO_4^{2-}$, pK_{10} = 13.2 $\pm$ 0.1, were found from plots against pH of the left side of the equations

$$\log(\epsilon - \epsilon_{TeO_3^-})/(\epsilon_{HTeO_4^{2-}} - \epsilon) = pH - pK_{8,9} \quad (26)$$

and

$$\log(\epsilon - \epsilon_{HTeO_4^{2-}})/(\epsilon_{TeO_4^{3-}} - \epsilon) = pH - pK_{10} \quad (27)$$

(Figure 8). ϵ is the extinction coefficient measured at varying pH. $\epsilon_{TeO_3^-}$, $\epsilon_{HTeO_4^{2-}}$, and $\epsilon_{TeO_4^{3-}}$, stand for the extinction coefficients of TeO_3^-, $HTeO_4^{2-}$, and TeO_4^{3-}, respectively. $pK_{8,9}$ was determined from measurements of ϵ at the wavelengths 325, 350, 375, 400, and 425 nm, pK_{10} from measurements of ϵ at 325 nm. Since the large base strength of TeO_4^{3-} precludes a direct determination of $\epsilon_{TeO_4^{3-}}$, pK_{10} was determined from eq 27 by adjusting $\epsilon_{TeO_4^{3-}}$ to $\epsilon_{TeO_4^{3-}}$ = 6400 M^{-1} cm^{-1} by trial

Tellurium(V). A Pulse Radiolysis Study

J. Phys. Chem. A, Vol. 105, No. 27, 2001 **6643**

TABLE 2: Standard Electrode Potentials

electrode process	$E°$/Volt[a]
$TeO_3^- + e^- = TeO_3^{2-}$	1.74
$TeO_3^- + H^+ + e^- = HTeO_3^-$	2.31
$HTeO_4^{2-} + e^- = TeO_3^{2-}$	1.50
$TeO_4^{3-} + H_2O + e^- = TeO_3^{2-} + OH^-$	1.45
$H_6TeO_6 + e^- = TeO_3^- + 3H_2O$	−0.40
$H_5TeO_6^- + e^- = HTeO_4^{2-} + 2H_2O$	−0.52
$H_4TeO_6^{2-} + e^- = TeO_4^{3-} + 3H_2O$	−0.66

[a] Estimated error ± 0.01 V.

and error until the required linear dependence on pH was obtained.

The determination of the rate constants for both pairs of forward and the reverse reactions 4, −4, and 5, −5 allows us to determine the standard Gibbs energy of formation of TeO_4^{3-}, $HTeO_4^{2-}$, and TeO_3^-. These may be calculated from

$$\Delta_f G_{ao}°(TeO_4^{3-}) = RT \ln(k_{-5}/k_5) + \Delta_f G_{ao}°(TeO_3^{2-}) + \Delta_f G_{ao}°(O^-) \quad (28)$$

$$\Delta_f G_{ao}°(HTeO_4^{2-}) = RT \ln(k_{-4}/k_4) + \Delta_f G_{ao}°(TeO_3^{2-}) + \Delta_f G_{ao}°(OH) \quad (29)$$

and

$$\Delta_f G_{ao}°(TeO_3^-) = RT \ln K_{8,9} + \Delta_f G_{ao}°(HTeO_4^{2-}) - \Delta_f G_{ao}°(H_2O) \quad (30)$$

The standard Gibbs energy of formation of $H_2TeO_4^-$ may be estimated from

$$\Delta_f G_{ao}°(H_2TeO_4^-) = \Delta_f G_{ao}°(HTeO_4^{2-}) + RT \ln K_{H_2TeO_4^-} \quad (31)$$

Taking $\Delta_f G_{ao}°(TeO_3^{2-}) = -383.4$ kJ/mol,[17] $\Delta_f G_{ao}°(O^-) = 95$ kJ/mol,[26] $\Delta_f G_{ao}°(OH) = 27$ kJ/mol,[26] and $\Delta_f G_{ao}°(H_2O) = -237.13$ kJ/mol,[27] and estimating $K_{H_2TeO_4} \cong 10^{-7}$[22] for the dissociation of $H_2TeO_4^-$, we find $\Delta_f G_{ao}°(TeO_4^{3-}) = -319$ kJ/mol, $\Delta_f G_{ao}°(HTeO_4^{2-}) = -394$ kJ/mol, $\Delta_f G_{ao}°(TeO_3^-) = -214$ kJ/mol, and $\Delta_f G_{ao}°(H_2TeO_4^-) \cong -434$ kJ/mol.
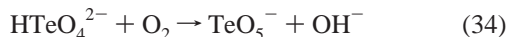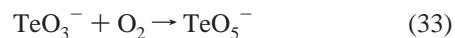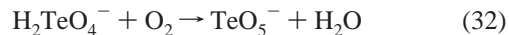
These results lead to $\Delta G° = 17$ kJ/mol for the hydration of TeO_3^- and, hence, to the estimate $K_8 \cong 10^{-3}$ for the equilibrium 8, −8, a value in agreement with the fact that reaction 8 was not observed.

The standard electrode potentials shown in Table 2 are calculated from the values of $\Delta_f G_{ao}°$ for the four Te(V) species and from published values of $\Delta_f G_{ao}°$ for the Te(IV) and Te(VI) species.[17]
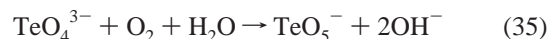
Reactions of Te(V) with O_2 and HCO_3^-. Te(V) species were found to react with O_2 under formation of a product having an absorption that increases with decreasing wavelength without reaching a maximum in the range (>250 nm) accessible with our instrument. The observable part of this spectrum resembles that of O_2^- [28] as well as those of SO_5^-,[29] the O_2-adduct of SO_3^-, and the O_2-adduct of As(IV).[23] Hence, with the reasonable assumption that an O_2-adduct of TeO_3^- (= TeO_5^-) would also have a spectrum similar to that of O_2^-, the observed spectrum suggests that the product is either O_2^- or TeO_5^-, the reduction of O_2 implied by both assignments being consistent with the high reduction power of the Te(V) species (Table 2). However,

the reaction between Te(V) and O_2 is very fast, which we take to suggest that TeO_5^- rather than O_2^- is the product.

The reactions of the Te(V) species $H_2TeO_4^-$, TeO_3^-, $HTeO_4^{2-}$, and TeO_4^{3-} with O_2 may be

$$H_2TeO_4^- + O_2 \rightarrow TeO_5^- + H_2O \quad (32)$$

$$TeO_3^- + O_2 \rightarrow TeO_5^- \quad (33)$$

$$HTeO_4^{2-} + O_2 \rightarrow TeO_5^- + OH^- \quad (34)$$

and

$$TeO_4^{3-} + O_2 + H_2O \rightarrow TeO_5^- + 2OH^- \quad (35)$$

The rate constants k_{33}, k_{34}, and k_{35}, for reactions 33, 34, and 35, were determined from measurements of the first-order rate constants for disappearance of Te(V) in N_2O-saturated 5×10^{-4} M tellurite solutions containing oxygen in the concentrations 1.9×10^{-4} M, 2.5×10^{-4} M, and 3.8×10^{-4} M O_2. At pH 7.9 the first-order rate constant for disappearance of Te(V) was found to be $(1.7 \pm 0.2) \times 10^5$ s^{-1} at 2.5×10^{-4} M O_2. Since the rate constant for the dehydration of $H_2TeO_4^-$ in 5×10^{-4} M tellurite is three times larger, we assume that the value measured pertains to the pseudo first-order constant of reaction 33. With this assumption we find $k_{33} = (6.8 \pm 0.8) \times 10^8$ M^{-1} s^{-1}. k_{34} (= $3.1 \pm 0.17 \times 10^8$ M^{-1} s^{-1}) was determined from measurements in solutions containing 1.9×10^{-4} M, 2.5×10^{-4} M, and 3.8×10^{-4} M O_2 at pH 11.1, at which pH $HTeO_4^{2-}$ is the predominant species. k_{35} (= $(2.5 \pm 0.3) \times 10^8$ M^{-1} s^{-1}) was determined from the value of k_{34} and the rate constant k (= $(2.8 \pm 0.3) \times 10^8$ M^{-1} s^{-1}) for disappearance of Te(V) determined in a solution containing 2.5×10^{-4} M O_2 at pH 13.3, where $HTeO_4^{2-}$ and TeO_4^{3-} are present in approximately equal concentrations.

Pseudo first-order rate constants for the disappearance of Te(V) in solutions containing CO_3^{2-} and HCO_3^- were measured in N_2O-saturated 10^{-2} M tellurite solutions and in 10^{-2} M O_2-free tellurate solutions. The product of the reaction was identified by its spectrum as CO_3^-.[30] The total concentration of carbonate, $[CO_3^{2-}] + [HCO_3^-]$, was varied between 10^{-2} M and 6×10^{-4} M. The fractions $x_{HCO_3^-} = [HCO_3^-]/([CO_3^{2-}] + [HCO_3^-])$ and $x_{TeO_3^-} = [TeO_3^-]/([HTeO_4^{2-}] + [TeO_3^-])$ were calculated from pH of the solutions and the pK values of HCO_3^- and TeO_3^-, taken as the values pertaining to infinite dilute solution (10.34 for HCO_3^- [27] and 9.97 for TeO_3^-) corrected by means of Güntelberg's formula for the activity coefficients of ions.[31]

In strongly alkaline solution (pH $\geq$ 13), where the dominant Te(V) species are $HTeO_4^{2-}$ and TeO_4^{3-}, no reaction was observed, indicating that CO_3^{2-} does not react at a measurable rate with $HTeO_4^{2-}$ and TeO_4^{3-}, in accordance with the fact that $\Delta G°$ for these reactions are positive.

Measurements in less alkaline solutions show that TeO_3^- is the only Te(V) species that reacts at a measurable rate with HCO_3^- and CO_3^{2-}. We find that the decay of the absorbance at 350 nm is of pseudo first order with a rate constant that for fixed $x_{HCO_3^-}$ (and $x_{TeO_3^-}$) is proportional to $[CO_3^{2-}] + [HCO_3^-]$. Further we find that the second-order constant, k_{36}, for the reaction of Te(V) with total carbonate ($CO_3^{2-} + HCO_3^-$) divided by $x_{TeO_3^-}$ varies linearly with $x_{HCO_3^-}$, indicating that $k_{36}/x_{TeO_3^-}$ may be expressed by

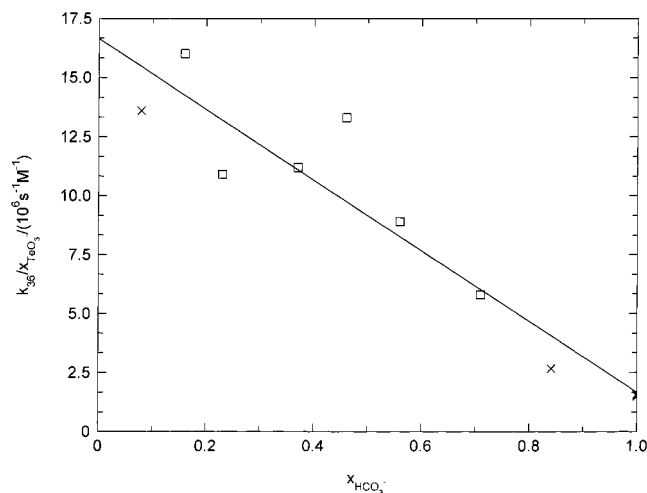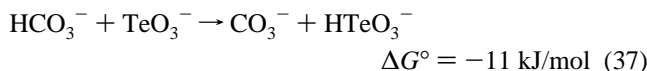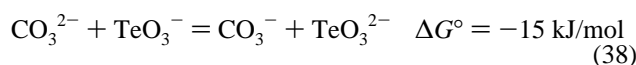$$k_{36}/x_{TeO_3^-} = k_{37}x_{HCO_3^-} + k_{38}(1 - x_{HCO_3^-}) \quad (36)$$

Figure 9. Determination of the rate constants k_{37} and k_{38} for oxidation HCO_3^- and CO_3^{2-} by TeO_3^-. $k_{36}/x_{TeO_3^-} = k_{37} \cdot x_{HCO_3^-} + k_{38}(1 - x_{HCO_3^-})$ is plotted against $x_{HCO_3^-}$. k_{36} is the pseudo-first-order rate constant for decay of absorbance at 350 nm in solutions containing HCO_3^- and CO_3^{2-} multiplied by $([HCO_3^-] + [CO_3^{2-}])$. $x_{TeO_3^-} = [TeO_3^-]/([TeO_3^-] + [HTeO_4^{2-}])$, $x_{HCO_3^-} = [HCO_3^-]/([HCO_3^-] + [CO_3^{2-}])$. □ and × are experimental points and the straight line is a linear least-squares fit to the experimental points. The points □ were measured in N_2O-saturated solutions containing $HTeO_3^-$ and TeO_3^{2-} in the total concentration 10^{-2} M, and in which the total concentration of HCO_3^- and CO_3^{2-} was varied between 5×10^{-3} M and 6×10^{-2} M. The points × were measured in Ar-saturated solutions containing H_6TeO_6, $H_5TeO_6^-$, and $H_4TeO_6^{2-}$ in the total concentration 10^{-2} M, and in which the total concentration of HCO_3^- and CO_3^{2-} was varied between 10^{-2} M and 2×10^{-2} M.

where k_{37} and k_{38} are the rate constants of

$$HCO_3^- + TeO_3^- \rightarrow CO_3^- + HTeO_3^-$$
$$\Delta G^\circ = -11 \text{ kJ/mol} \quad (37)$$

and

$$CO_3^{2-} + TeO_3^- = CO_3^- + TeO_3^{2-} \quad \Delta G^\circ = -15 \text{ kJ/mol} \quad (38)$$

respectively. ΔG° for reactions are calculated taking the standard electrode potential of CO_3^-/CO_3^{2-} equals 1.59 V.[32]

Figure 9 shows a plot of $k_{36}/x_{TeO_3^-}$ against $x_{HCO_3^-}$. From a linear least-squares fit to the experimental points we find $k_{37} = 1.6 \times 10^6$ M^{-1} s^{-1} and $k_{38} = 1.7 \times 10^7$ M^{-1} s^{-1}. We note that k_{38} is much larger than k_{37}, reflecting that reaction 37 takes place by hydrogen atom transfer, and reaction 38 by electron transfer.

Comparison of the Oxoradicals of S(V), Se(V), and Te(V). The only four-coordinated Se(V) oxoradical observed in aqueous solution is $HSeO_4^{2-}$.[6] This species is detected only in strongly alkaline solution (pH > 13) indicating an extremely low acid strength, which of cause precludes the detection in aqueous solution of its corresponding base, SeO_4^{3-}. This species, however, has been observed in X-ray-irradiated crystals containing SeO_4^{2-}.[10]

The low acid strength of $HSeO_4^{2-}$ as compared to that of $HTeO_4^{2-}$, and the fact that $H_2TeO_4^-$ is observed whereas $H_2SeO_4^-$ is not, may be rationalized by comparing the set of reactions 8, −8, 9, and −9 with the corresponding set

$$SeO_3^- + H_2O \rightleftarrows H_2SeO_4^- \rightleftarrows HSeO_4^{2-} + H^+$$
$$(39),(-39),(40),(-40)$$
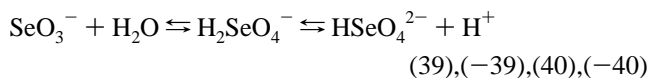
Denoting the standard Gibbs energy changes for the total

TABLE 3: Standard Electrode Potentials of SO_3^-, SeO_3^-, and TeO_3^-

electrode process	E_o/Volt	ref
$SO_3^- + e^- = SO_3^{2-}$	0.73 ± 0.01	1
$SeO_3^- + e^- = SeO_3^{2-}$	1.68 ± 0.01	6
$TeO_3^- + e^- = TeO_3^{2-}$	1.74 ± 0.02	this work
$SO_4^{2-} + 2H^+ + e^- = SO_3^- + H_2O$	-0.91 ± 0.01	1
$SeO_4^{2-} + 2H^+ + e^- = SeO_3^- + H_2O$	-0.03 ± 0.01	6
$H_4TeO_6^{2-} + 2H^+ + e^- = TeO_3^- + 3H_2O$	-0.70 ± 0.02	this work

reactions by ΔG° (8,9) and ΔG° (39,40), respectively, we have

$$\Delta G^\circ(39,40) - \Delta G^\circ(8,9) = -RT \ln K_{39,40} + RT \ln K_{8,9} \quad (41)$$

Taking the acid constants K_{41} and K_9 of $H_2SeO_4^-$ and $H_2TeO_4^-$ to be equal and assuming, moreover, that the rate constant of the uncatalyzed hydration of SeO_3^- is equal to that of TeO_3^-, i.e., $k_{39} = k_8$ we find

$$-RT \ln K_{39,40} + RT \ln K_{8,9} = \Delta G^\circ(39) - \Delta G^\circ(8) = RT \ln k_{-39}/k_{-8} \quad (42)$$

for the difference between the standard Gibbs energy of hydration of SeO_3^- and of TeO_3^-.

Setting $K_{39,40} = 10^{-14}$,[6] $K_{8,9} = 10^{-10}$, and $k_{-8} = k_6 \sim 10^4$ s^{-1} as determined above for the uncatalyzed dehydration of $H_2TeO_4^-$, we find $k_{-39} \sim 10^7$ s^{-1} for the uncatalyzed dehydration of $H_2SeO_4^-$, a value that would make $H_2SeO_4^-$ impossible to detect with the apparatus used.[6]

In contrast to Se(V) and Te(V), S(V) apparently cannot form four-coordinated oxoradicals. Thus the species SO_4^{3-} is inherently unstable: electron attachment to SO_4^{2-} in solid K_2SO_4 leads to immediate dissociation into O^- and SO_3^{2-} even at cryogenic temperatures.[33] Moreover, the fact that sulfate in contrast to selenate and tellurate is inert toward reduction by the hydrated electron[16] suggests that this dissociative state (SO_4^{3-}) lies high in energy. Consequently, whereas the oxidation of selenite and tellurite by O^-/OH seems to take place by addition to the selenium or tellurium atom, this type of process does not appear feasible for sulfite.

The standard electrode potentials of SO_3^-, SeO_3^-, and TeO_3^- are compiled in Table 3. As apparent from the table, the redox properties do not change smoothly on going from SO_3^- to TeO_3^-. Thus, as oxidants, SeO_3^- and TeO_3^- are equally strong and much stronger than SO_3^-. On the other hand, as reducing agents, SO_3^- and TeO_3^- are of similar strength and much stronger than SeO_3^-. These differences are reflected in the reactions with O_2 and with HCO_3^- and CO_3^{2-}: SeO_3^- and TeO_3^- both oxidize HCO_3^-/CO_3^{2-} to CO_3^-, SO_3^- does not; SO_3^- and TeO_3^- both reduce O_2, whereas no reaction of O_2 with SeO_3^- has been observed.[6]

References and Notes

(1) Neta, P.; Huie, R. E. *Environ. Health Perspect.* **1985**, *64*, 209.
(2) Stanbury, D. M. *Adv. Inorg.Chem.* **1989**, *33*, 69.
(3) Das, T. N.; Huie, R. E.; Neta, P. *J. Phys. Chem. A* **1999**, *103*, 3581.

Tellurium(V). A Pulse Radiolysis Study

J. Phys. Chem. A, Vol. 105, No. 27, 2001 **6645**

(4) Waygood, S. J.; McElroy, W. J. *J. Chem. Soc., Faraday Trans.* **1992**, *88*, 1525.

(5) Huie, R. E.; Neta, P. *J. Phys. Chem.* **1984**, *88*, 5665.

(6) Kläning, U. K.; Sehested, K. *J. Phys. Chem.* **1986**, *90*, 5460.

(7) Jonah, C. D.; Miller, J. R.; Matheson, M. S. *J. Phys. Chem.* **1977**, *81*, 1618.

(8) Anbar, M.; Hart, E. J. *Adv. Chem. Ser.* **1968**, *81*, 79.

(9) Adams, G. E.; Boag, J. W.; Michael, R. D. *Trans. Faraday Soc.* **1965**, *61*, 1674.

(10) Hukuda, K.; Hanafuse, H.; Kawano, T. *J. Phys. Jpn.* **1974**, *36*, 1043.

(11) Matsuki, K. *J. Phys. Jpn.* **1992**, *61*, 377.

(12) Siebert, H. *Z. Anorg. Allg. Chem.* **1954**, *275*, 225.

(13) Rabani, R.; Matheson, M. S. *J. Phys. Chem.* **1966**, *70*, 761.

(14) Schwarz, H. A. *J. Chem. Educ.* **1981**, *58*, 101.

(15) Draganič, Z. D.; Draganič, L. G. *J. Phys. Chem.* **1973**, *77*, 765.

(16) Buxton, G. V.; Greenstock, C. L.; Helman, W. P.; Ross, A. B. *J. Phys. Ref. Data* **1988**, *17*, 197.

(17) McPhail, D. C. *Geochim. Cosmochim. Acta* **1995**, *5*, 851.

(18) Mendes, P. *Comput. Appl. Biosci.* **1993**, *9*, 563.

(19) Mendes, P. *Trends. Biochem. Sci.* **1997**, *22*, 361.

(20) Mendes, P. *Bioinformatics* **1998**, *14*, 869.

(21) Pauling, L. *General Chemistry*, 3rd ed.; W. H. Freeman: San Francisco, 1970.

(22) Eigen, M.; Kruse, W.; Maas. G.; De Mayer, L. *Prog. React. Kinet.* **1964**, *2*, 285.

(23) Kläning, U. K.; Bielski, B. H. L.; Sehested, K. *Inorg. Chem.* **1989**, *28*, 2717.

(24) Kläning, U. K.; Sehested, K.; Wolff, T. *J. Chem. Soc., Faraday Trans.* **1981**, *77*, 1707.

(25) Kläning, U. K.; Sehested, K.; Wolff, T.; Appelman, E. H. *J. Chem. Soc., Faraday Trans.* **1982**, *78*, 1539.

(26) Kläning, U. K.; Sehested, K.; Holcman, J. *J. Phys. Chem.* **1985**, *89*, 760.

(27) Wagmann, D. D.; Evans, W. H.; Parker, V. B.; Schumm, R. H.; Halow, I.; Baley, S. M.; Churney, K. L.; Nutall, R. L. *J. Phys. Ref. Data* **1982**, *11* (Suppl. 2).

(28) Bielski, B. H. J.; Cabelli, D. E.; Arudi, R. L. *J. Phys. Ref. Data* **1985**, *14*, 1041.

(29) Hayon, E.; Treinin, A.; Wilf, J. *J. Am. Chem. Soc.* **1972**, *94*, 47.

(30) Weeks, J. L.; Rabani, J. *J. Phys. Chem.* **1966**, *70*, 2100.

(31) Robinson, R. A.; Stokes, R. A. *Electrolyte Solutions*, 2nd ed. (revised); Butterwords: London, 1970.

(32) Huie, R. E.; Clifton, C, L.; Neta, P. *Radiat. Phys. Chem.* **1991**, *38*, 477.

(33) Byberg, J. R. *J. Chem. Phys.* **1986**, *84*, 6083.